Carbohydrate Polymers 88 (2012) 1364–1372

Contents lists available at SciVerse ScienceDirect

Carbohydrate Polymers

journal homepage: www.elsevier.com/locate/carbpol

Synthesis and characterization of methylcellulose/PVA based porous composite

Anuj Kumar[a], Yuvraj Singh Negi[a,*], Nishi Kant Bhardwaj[a], Veena Choudhary[b]

[a] Polymer Science and Technology Program, DPT, Indian Institute of Technology Roorkee, Saharanpur Campus, Saharanpur 247001 (U.P.), India
[b] Centre for Polymer Science and Engineering, Indian Institute of Technology Delhi, New Delhi 110016, India

ARTICLE INFO

Article history:
Received 23 December 2011
Received in revised form 7 February 2012
Accepted 9 February 2012
Available online 18 February 2012

Keywords:
Sugarcane bagasse
Porosity
Methylcellulose
Polyvinyl alcohol
Composite

ABSTRACT

The synthesis of methylcellulose (MC) from chemically purified cellulose extracted from sugarcane bagasse was carried out with dimethyl sulfate (DMS) in the presence of sodium hydroxide and acetone as solvent under heterogeneous conditions and the degree of substitution (DS) was determined as 1.44. 3D porous composite of methylcellulose/polyvinyl alcohol (MC/PVA) was prepared by freeze drying process. The synthesized products were characterized by FE-SEM, FTIR, ^{1}H NMR and XRD. Porosity was calculated as 86% and the binary image, histogram of pores distribution of MC/PVA porous composite were investigated by ImageJ processing technique which shows the roughness of the topographical structure. Synthesized methylcellulose enhances the value to this abundant agro-industrial residue and may extend its range of biomedical applications.

1. Introduction

Sugarcane bagasse is an abundant agro-industrial by-product worldwide and is used in many different applications (Pereira et al., 2011; Ripoli, Molina, & Ripoli, 2000; Tita, de Paiva, & Frollini, 2002). Sugarcane bagasse consists of cellulose 43.8%, hemicellulose 28.6%, lignin 23.5%, ash 1.3%, and other components 2.8% (Sun, Sun, & Sun, 2004; Viera et al., 2007). Lignin serves as a cementing matrix for cellulose fibrils and hemicellulose molecules (Chakraborty, Chowdhury, & Saha, 2011). Cellulose is a polydisperse linear homopolymer consisting of regio-enantioselective β-1,4-linked anhydro-D-glucose units. Each glucose monomer contains three reactive hydroxyl (—OH) groups at C-2, C-3 and C-6 atoms, however, it is relatively inert because of extensive intra- and intermolecular hydrogen bonding where three —OH groups of each cellulose unit are responsible for most of the interactions with organic and inorganic substances (Chakraborty et al., 2011; Habibi, Lucia, & Rojas, 2010).

Therefore, chemically purified cellulose from sugarcane bagasse shows semi-crystalline behavior and is insoluble in water and common organic solvents. In spite of its high crystallinity, cellulose decomposes before it undergoes melt flow. Therefore, cellulose is generally converted into derivatives such as ethers and esters because these derivatives are much more soluble. Different cellulose derivatives have been produced from the chemically purified cellulose of sugarcane bagasse. This may be observed on the production of carboxymethylcellulose (Morais & Campana Filho, 1999), Cellulose acetate (Rodrigues Filho et al., 2000), on the studies related to the production of methylcellulose (Filho et al., 2007; Viera, Meireles, de Assuncao, & Rodrigues Filho, 2004; Viera et al., 2007).

Etherification of cellulose is one of the most important routes of cellulose derivatization (Bhatt, Gupta, & Naithani, 2011) and methylcellulose is one of the important cellulose ethers (Donges, 1990; Just & Majewicz, 1985; Nikitin, 1962). Methylcellulose presents an increase in thermal stability and solubility in water associated with the increase of the degree of substitution (DS), which improve the commercial applicability of the polymer (Filho et al., 2007). Several products of considerable commercial importance can be developed from methylcellulose. For example, it may be used as thickener in the food industry (Reibert & Conklin, 1999), as matrix for controlled release of drugs in the pharmaceutical industry (Mitchel et al., 1993), as admixture for concrete in civil construction (Fu & Chung, 1996). The use of methylcellulose in these activities depends on its solubility in water, and consequently, on the degree of substitution (DS) of the polymer. When this polymer is prepared with a DS between 1.4 and 2.0, cold or hot water may be used to produce solutions or dispersions in low concentration (Zohuriaan & Shokrolahi, 2004). For DS higher than 2.0, the polymer shows solubility in organic solvents (Filho et al., 2007).

Polyvinyl alcohol (PVA) is a well known biologically friendly, non-toxic, semicrystalline synthetic polymer with properties such as water solubility, biodegradability and biocompatibility, and therefore, it finds use in a broad spectrum of applications (Chhatri, Bajpai, Sandhu, Jain, & Biswas, 2011; Finch, 1973; Peresin, Habibi, Zoppe, Pawlak, & Rojas, 2010), like biomedical applications such

* Corresponding author. Tel.: +91 132 2714328.
E-mail address: yuvrajnegi@gmail.com (Y.S. Negi).

0144-8617/$ – see front matter © 2012 Elsevier Ltd. All rights reserved.
doi:10.1016/j.carbpol.2012.02.019

as synthetic vitreous body (Inoue et al., 1992), artificial pancreas (Giusti, Lazzeri, & Barbani, 1993; Young, Chuang, Yao, & Chen, 1998), wound dressings, artificial skin, and cardiovascular devices (Burczak, Gamian, & Kochman, 1996; Hassan & Peppas, 2000a, 2000b; Hoffman, 2002; Lee & Mooney, 2001; Razzak, Zainuddin, Dewi, Lely, & Taty, 1999; Wan, Campell, Zhang, Hui, & Boughner, 2002).

In the present work, we synthesized methylcellulose from sugarcane bagasse cellulose with dimethyl sulfate (DMS) in the presence of sodium hydroxide and acetone as solvent in heterogeneous conditions and fabricated porous composite of this methylcellulose and polyvinyl alcohol (PVA) by freeze drying. Information on structure and morphology was carried out using Fourier transform infra-red spectroscopy (FTIR), X-ray diffractometry (XRD), proton nuclear magnetic resonance (^{1}H NMR) and scanning electron microscopy (SEM). Image analysis of synthesized products was done using ImageJ software to investigate the length, diameter of the fibers, and apparent surface topography of the porous composite.

2. Materials and methods

2.1. Materials

Sugarcane bagasse was provided by a local sugar factory (Uttar Pradesh, India). After drying in sunlight, it was ground and sieved under 30 mesh screens. Bagasse was dried in oven at 105 °C for 3 h and stored at room temperature in air tight polybag. PVA supplied by Fisher Scientific with 85–89 degree of hydrolysis, benzene, methanol, sodium chlorite, acetic acid, potassium hydroxide, sodium hydroxide, dimethyl sulfate, acetone were of analytical grade. Distilled water was used throughout the experiment.

2.2. Methods

2.2.1. Isolation of chemically purified cellulose

Chemical purification of sugarcane bagasse was performed according to the methods of (Abe, Iwamoto, & Yano, 2007; Abe & Yano, 2009; Chen et al., 2011). Sugarcane bagasse (5.0 g) was first dewaxed in a Soxhlet apparatus with a 2:1 (v/v) mixture of benzene and methanol for 5–6 h. Lignin in the bagasse was then removed by using acidified sodium chlorite solution at 75 °C for 1 h. The process was repeated 3–4 times until the product became white. After this delignification process, the product was treated in 2 wt% KOH at 85–90 °C for 2 h to remove hemicellulose with residual starch, and pectin. To give highly chemically purified cellulose, the product was further treated with acidified sodium chlorite solution at 75 °C for 1 h and then treated with 5 wt% potassium hydroxide at 85–90 °C for 2 h. After the chemical treatments, the product was filtered and rinsed with distilled water until the filtrate pH was neutral. Finally the, product was dried in oven at 105 °C for 6 h followed by storage in air tight polybags.

2.2.2. Methylation of chemically purified cellulose

Chemically purified cellulose was methylated according to the method reported by Mansour, Nagaty, and El-Zawawy (1994), Viera et al. (2007), and Filho et al. (2007), with some modification. The process is as follows: chemically purified cellulose (1.0 g) was mercerized by using a 50% sodium hydroxide solution for 1 h at room temperature. The excess of the NaOH solution was squeezed out and acetone (9 mL) was added as a solvent. Dimethyl sulfate (3 mL) was added dropwise and the reaction was allowed to proceed at 50 °C with gentle and constant stirring. After 1.5 h of reaction, the system was filtered and fresh reactants (DMS and acetone) were added, maintaining the same previous proportions for the next 1.5 h of reaction. At the end of the reaction, the material was neutralized by 10% acetic acid solution, filtered on a sintered crucible, and then washed with acetone. Methylcellulose was dried in an oven at 55 °C for 6 h.

2.2.3. Fabrication of methylcellulose/polyvinyl alcohol (MC/PVA) as porous composite

0.5 g of methylcellulose was soaked in distilled water for 5 h for swelling and then stirred using magnetic stirrer at 80 °C temperature for 7 h for dissolution and the final solution was obtained by removing un-reacted fibrils which were not dissolved. 2 g of poly(vinyl alcohol) was dissolved in distilled water at 65 °C for 3 h. Further both the solutions were mixed together with constant stirring for 2 h and the obtained solution was kept in deep freezer at −40 °C for 7 h and the freeze drying was done at −40 °C for 2 days using Lyodel (Delvac Pumps Pvt. Ltd., India).

3. Characterization methods

3.1. Measurement of chemical composition

The chemical composition of the untreated sugarcane bagasse fibers was measured according to Technical Association of Pulp and Paper Industry (TAPPI) Standard Test Methods. The lignin content was calculated by the reaction with sulfuric acid, using a standard method (TAPPI-T222 om-98). The holocellulose (cellulose + hemicelluloses) content was determined as described in TAPPI-T19 m-54. Chemically purified α-cellulose content was then calculated after further treatment of the fibers with NaOH to remove the hemicelluloses. Fiber morphology of the sugarcane bagasse and chemically purified cellulose fibers was investigated using the software ImageJ image processing.

3.2. Determination of degree of substitution (DS)

The degree of substitution (DS) of methylcellulose was calculated by the following formula (Bhatt et al., 2011).

$$\text{Degree of substitution (DS)} = \frac{\%\,\text{Weight increase} \times \text{mol. wt. of anhydroglucose unit}}{\text{Mol. wt. of methyl unit } (-CH_3) \times 100}$$

3.3. Field emission scanning electron microscopy (FE-SEM)

The surface morphology of the fibers after chemical treatments and preparation of the porous composite was examined using field emission electron microscopy (FE-SEM) (FEI Quanta 200 F) microscope with an accelerating voltage of 10–15 kV. Before examination, the samples were sprayed with a fine layer of gold by an ion sputter coater with a low deposition rate.

3.4. Fourier transform-infra red (FTIR) spectroscopy

FTIR allows the measurements of variations on samples because of the chemical treatments. The chemical structure of chemically purified cellulose from sugarcane bagasse, polyvinyl alcohol, and modification of cellulose by methylation was evaluated by FTIR spectroscopy using a Nicolet spectrophotometer. Samples were oven dried at 105 °C for 4 h, mixed with KBr in a ratio of 1:200 (w/w) and pressed under vacuum to form pellets. FTIR of the samples were recorded in the transmittance mode.

Table 1
Chemical composition and fiber morphology of the fibers.

Chemical components	Sugarcane bagasse
Holocellulose (%)	72.2
α-Cellulose (%)	49.7
Hemicellulose (%)	22.5
Total lignin (%)	24.7
Ashes/other components (%)	3.1
Moisture (%)	9.7

Fiber morphology	Sugarcane bagasse	Chemically purified cellulose
Length (μm)	500–2000	100–500
Diameter (μm)	50–400	10–25
Aspect ratio (L/D)	10–5	10–20

3.5. Proton nuclear magnetic resonance (^{1}H NMR)

^{1}H NMR spectra were recorded on a Bruker DPX-300 spectrometer operating at 300 MHz at room temperature. Methylcellulose was dissolved in D_2O and tetramethylsilane (TMS) was the internal standard.

3.6. X-ray diffraction (XRD)

The physical structure of the samples were evaluated by X-ray diffraction (XRD) using a Bruker AXS D8 Advance diffractometer with a scanning rate of 5 °C per min with Cu Kα radiation source (λ = 1.54060 Å) operating at 40 kV and 30 mA. The patterns were obtained over the angular range 5–70°.

3.7. Image analysis

The dimensions of the fibers and binary image, the histogram, and interactive 3D surface plot of pores distribution of porous composite were measured by using ImageJ software (Java version) image processing.

3.8. Porosity

The porosity of freeze dried porous composite was evaluated by using a gravimetric measurement. The thicknesses of the samples were measured using a Vernier Callipers (PREISSER-DIGI-MET). The porosity (%) was calculated by the following formula.

$$\text{Porosity}\,(\%) = \left[1 - \left(\frac{d_{app}}{d_p}\right)\right] \times 100$$

where d_{app} is the apparent density of the porous composite and d_p is the density of non-porous composites.

4. Results and discussion

4.1. Chemical composition and morphology of the fibers

The results obtained on chemical composition of the bagasse fibers and fiber morphology of the bagasse and purified cellulose are given in Table 1. Our morphological results of fibers support the previous results reported by Pereira et al. (2011).

4.2. Surface morphology

To confirm the changes in morphology of the cellulose fiber by the effect of the chemical treatments, samples were analyzed by field emission scanning electron microscopy. In Fig. 1(i) (A and B), SEM images show as received (30 mesh screen) sugarcane bagasse fibers, providing evidence of surface layers with a high percentage of extractives on the fibers. When delignification of sugarcane bagasse fibers was done with acidic sodium chlorite solution, a definitive change in the morphological structure of the sugarcane bagasse, which shows removal of the extractives from surface fibers, was apparent.

Table 2
Main absorption bands in sugarcane bagasse and chemically purified cellulose (Colom, Carrillo, Nogues, & Garriga, 2003; Pereira et al., 2011; Viera et al., 2007).

Wave number (cm^{-1})		Vibration
Sugarcane bagasse	Chemically purified cellulose	
3426	3426	O—H stretching
2922	2900	C—H stretching of CH_2 and CH_3 groups.
1730	–	C=O un-conjugated stretching of acetyl or carboxylic acid (xylans)
–	1648	H—O—H bending (water)
1634	–	C=O stretching with aromatic ring
1620–1595	–	C=C stretching of aromatic ring (lignin)
(1512)	–	C=C stretching of aromatic ring (lignin)
1429	1432	CH_2 bending
1376	1374	C—H deformation
1335	1335	O—H in plane bending (cellulose)
(1250)	(1250)	C—O stretching of ether linkage
1166	1162	C—O—C asymmetric bridge stretching (cellulose)
1062	1062	C—O symmetric stretching of primary alcohol
904	896	β-Glucosidic linkages between the sugar units
670	672	C—OH out-of-plane bending (cellulose)

Delignification process provides relatively cleaner surfaces, which is consistent with the removal of wax, pectin, lignin, and hemicelluloses, while typical vegetable cells, parenchyma, and pits could be observed in the sodium chlorite treated samples as shown in Fig. 1(i) (C and D). On the other hand, applying whole chemical treatment as with 2 wt% KOH, acidified sodium chlorite, and 5 wt% KOH, respectively, the fibers exhibited bundles of round, fine, long, and smooth surfaced fibers. This can be seen in Fig. 1(i) (E and F).

Fig. 1(ii) (A and B) shows the scanning electron micrographs of chemically purified α-cellulose and methylcellulose fibers, respectively. The surface topography of chemically purified α-cellulose was found to be even and smooth while modification of α-cellulose to methylcellulose showed significant changes on the surface of cellulose fibers where evenness and smoothness on the fiber surface was not observed. This is evidence of probable chemical modification.

4.3. Structural analysis

4.3.1. Fourier transform-infra red (FTIR) spectroscopy analysis

The major differences in relation to the functional groups in the sugarcane bagasse and in chemically purified cellulose may be observed on the FTIR spectra at the region from 4000 to 400 cm^{-1} as shown in Fig. 2(A). The absorption bands at 1730, 1620, 1595 and 1512 cm^{-1}, which are attributed to the functional groups that are present in the lignin that is associated to the sugarcane bagasse before the process of chemical purification for removing the lignin, are not observed on the spectrum of chemically purified cellulose and two other absorption bands which must be emphasized are at 1512 and 1250 cm^{-1}. The main absorption band in sugarcane bagasse and chemically purified cellulose is shown in Table 2.

The band at 1512 cm^{-1} is not present and the band at 1250 cm^{-1} is drastically reduced on the chemically purified cellulose FTIR

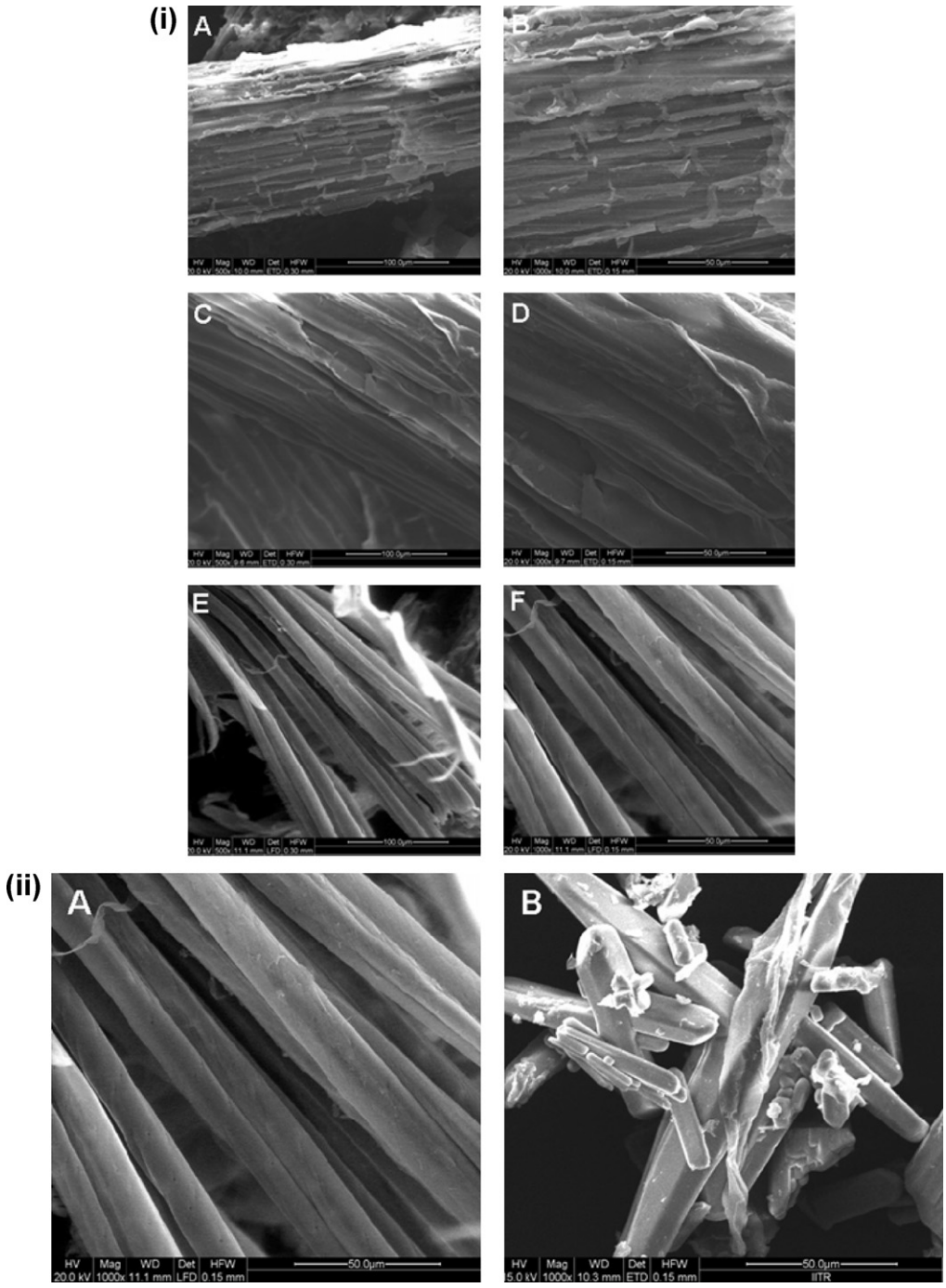

Fig. 1. SEM images of (i): (A and B) sugarcane bagasse (500×, 1000×); (C and D) de-lignified sugarcane bagasse (500×, 1000×); (E and F) chemically purified cellulose (500×, 1000×) and (ii): (A) bundles of fibril cellulose, magnification (1000×); (B) randomly substituted methylcellulose, magnification (1000×) (scale bar represents 50 μm).

which indicates that the most of the lignin was removed by the chemical treatment (Viera et al., 2007).

Synthesized methylcellulose is often comprised of un-reacted fibrils, methylcellulose with an inhomogeneous distribution of the methoxyl group, and salts. The chemical modification of chemically purified cellulose by methylation reaction gives some changes to the structure of cellulose between region from 3600 to 2700 cm^{-1} and from 1500 to 800 cm^{-1}. In the first region, the ratio between the intensities of O—H stretching band (~3400 cm^{-1}) and the C—H stretching band (2900 cm^{-1}) is lower and alteration of the shape of the band in approximately 2918 cm^{-1} and the displacement of this to higher frequencies in the spectrum of methylcellulose as compared to chemically purified cellulose.

FTIR spectral characterization was used to study the functional group modifications and to observe the DS of methylcellulose qualitatively during synthesis. Methylcellulose was produced via alkali cellulose which was further used for methylation by DMS as a methylating agent through the following general substitution mechanism:

$$\text{Cell-OH} + \text{NaOH} \rightarrow \text{Cell-ONa} + H_2O,$$

$$\text{Cell-ONa} + CH_3O{-}SO_2{-}OCH_3 \rightarrow \text{Cell-}(OCH_3)_3 + Na_2SO_4.$$

Fig. 2(B) shows the FTIR spectra of chemically purified cellulose and methylcellulose. The spectra were standardized at 1110 cm^{-1} and assigned to C—O—C stretching within an anhydroglucose

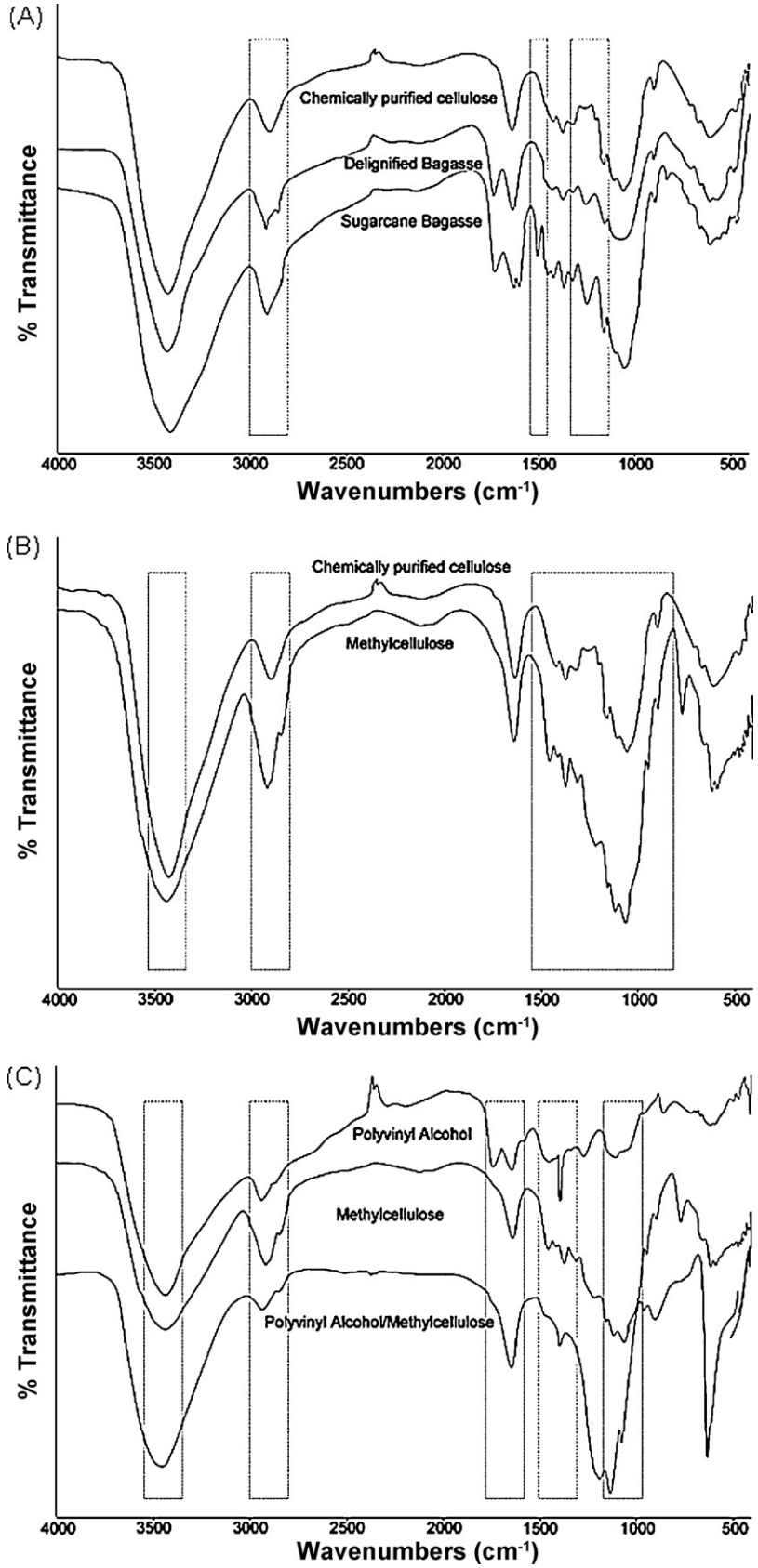

Fig. 2. FTIR spectra of (A) chemical purified cellulose, delignified bagasse, and sugarcane bagasse; (B) chemical purified cellulose and methylcellulose; (C) polyvinyl alcohol (PVA-85-89), methylcellulose, and polyvinyl alcohol/methylcellulose porous composite.

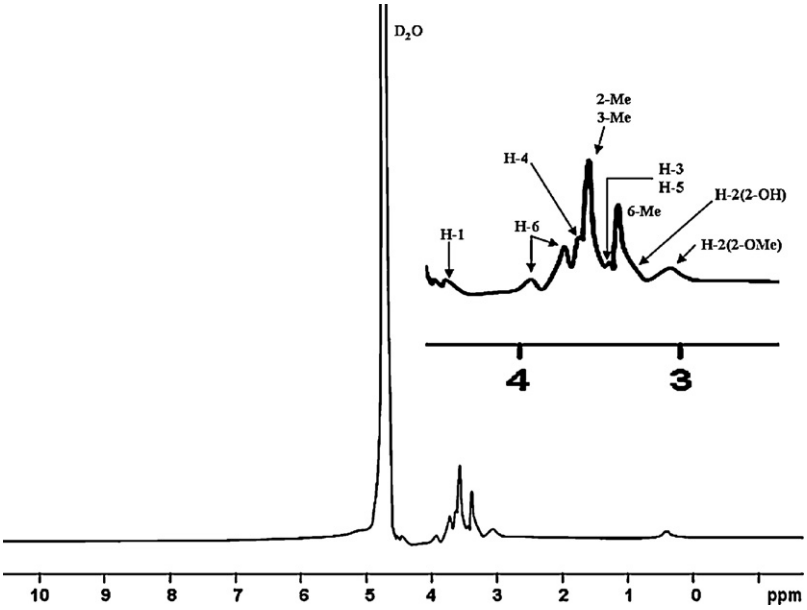

Fig. 3. ^{1}H NMR spectrum (in D_2O) of the 2,3,6-tri-*O*-methylcellulose obtained from sugarcane bagasse cellulose.

ring (Sekiguchi, Sawatari, & Kondo, 2003). The main differences between the spectra of methylated samples and the spectrum of purified cellulose are seen at the region from 3600 to 2700 cm^{-1}. The main difference between methylated sample and cellulose is the modification in absorbance intensity of the bands at about 3500 cm^{-1} assigned to O—H stretching and 2900 cm^{-1} assigned to C—H stretching. We can observe that the ratio of the absorption intensities of C—H stretching and O—H stretching increases in methylated cellulose samples. As DS increased, a larger ratio between C—H and O—H absorption bands was observed. In addition, the increase in water solubility of methylcellulose may indicate a higher DS for this sample.

Fig. 2(B) shows the detailed FTIR spectra of chemically purified cellulose and methylcellulose from 1500 to 500 cm^{-1}. This region is particularly sensitive to structural changes such as the increase or decrease in the degree of order; alteration of the hydrogen bond pattern during mercerization and synthesis, and to the kind of the produced cellulosic derivative, considering not only the kind of replacing group but also its degree of substitution (DS) (Sekiguchi et al., 2003; Zhbankov, 1966). The infrared spectra of methylcellulose presents especially the bands in 1460, 1380, 1320 and 950 cm^{-1} (Zhbankov, 1966). All of these bands are clearly present in methylcellulose spectrum which is characteristic of a more amorphous pattern and of a possible heterogeneity on the distribution of the substituting groups in the polymeric chain. However, methylcellulose spectra presents some differences when compared to the original cellulose and may indicate the existence of a mixture of modified cellulose (methylated) with unmodified cellulose.

Fig. 2(C) shows the FTIR spectra of PVA (PVA-85-89), methylcellulose (MC), and polyvinyl alcohol/methylcellulose blend. For PVA (PVA-85-89), the large band observed between 3600 and 3200 cm^{-1} are linked to the stretching O—H from the intermolecular and intramolecular hydrogen bonds, the vibrational band observed between 2840 and 3000 cm^{-1} refers to the stretching C—H from alkyl groups and the peaks between 1750 and 1620 cm^{-1} are due to the stretching C=O and C—O from acetate group remaining from PVA, peaks for C—O at 1141 cm^{-1} (crystallinity) and for C—O—C at 1150–1085 cm^{-1}, bending vibration related to CH_2 groups at 1461–1417 cm^{-1} (Mansur, Sadahira, Souza, & Mansur, 2008). The FTIR spectra of the polyvinyl alcohol/methylcellulose

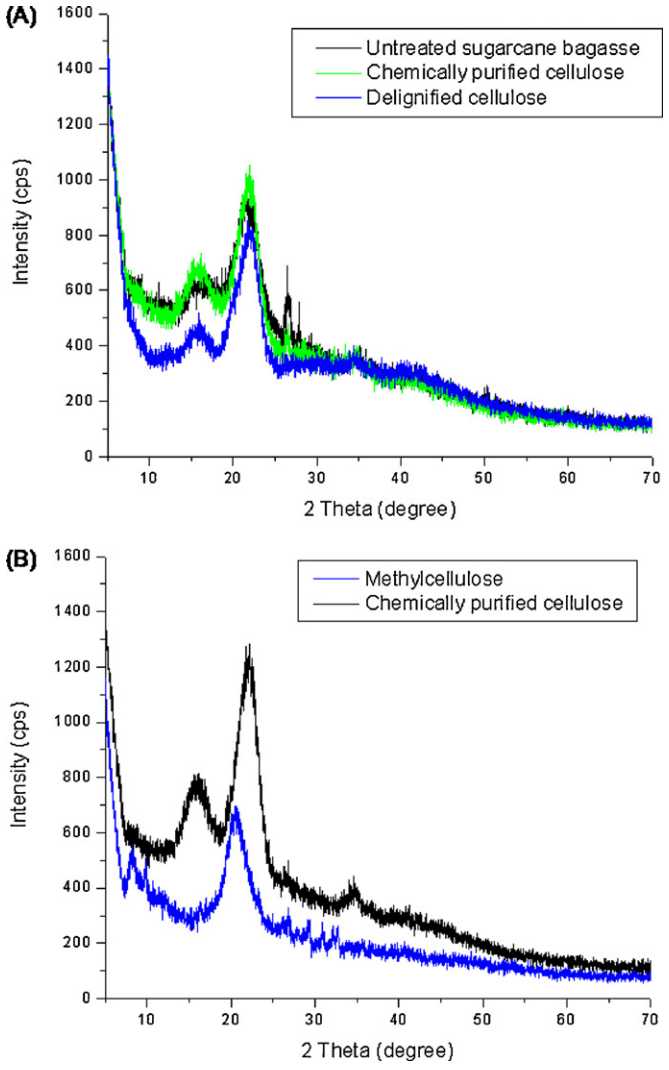

Fig. 4. (A) X-ray diffraction curve of untreated sugarcane bagasse, de-lignified cellulose, and chemically purified cellulose; (B) X-ray diffraction curve of chemically purified cellulose and synthesized methylcellulose.

porous scaffold, shows mixed major peaks of PVA (PVA-85-89) and methylcellulose (as discussed above) are observed, which confirms the blending of both polymers.

4.3.2. Proton nuclear magnetic resonance (^{1}H NMR)

^{1}H NMR is a powerful tool for evaluating the chemical structure of the compound in supporting the data of FTIR values of functional group. From Fig. 3, it was determined that the synthesized product is randomly substituted 2,3,6-tri-*O*-methylcellulose (Sekiguchi, Sawatari, & Kondo, 2002). In ^{1}H NMR spectra of methylcellulose in D_2O solvent, the proton signals overlap with each other because of the conformation changes of the structure. The signals due to 2-Me and 3-Me at 3.58 ppm were not well distinguished while H-1 and 6-OH became single signal because of deuteration of three unsubstituted hydroxyl (—OH) groups (2-, 3-, and 6-OH) of methylcellulose into OD.

The signals for H-4, H-6, H-1, H-3 and H-5 were appeared at 3.62 ppm, 3.7 ppm and 3.91 ppm, 4.51 ppm, 3.4–3.5 ppm, respectively. The signal of substituted methyl groups at the C(6) position in commercial methylcellulose (randomly substituted methylcellulose) are observed at 3.4 ppm (Sekiguchi et al., 2002) which supports our results.

4.4. X-ray diffraction (XRD) studies

The XRD results of untreated sugarcane bagasse, de-lignified cellulose, and chemically purified cellulose were shown in Fig. 4(A) and basically all the diffractogram showed a peak around $2\theta = 16.5^\circ$ and 22.5°, which are believed to represent the typical cellulose-I structure (Chen et al., 2011; Nishiyama, Langan, & Chanzy, 2002; Nishiyama, Sugiyama, Chanzy, & Langan, 2003).

The crystallinity of the samples was calculated according to amorphous subtraction method (Park, Baker, Himmel, Parilla, & Johnson, 2010). The crystallinity in the original untreated sugarcane bagasse was 35.6% but increased in case of chemically purified cellulose was 63.5% because of removal of hemicelluloses and lignin, which exist in the amorphous regions. This large increase is because of the high hemicellulose and lignin contents.

Table 3
Crystallinity percentage at different stages of chemical treatments.

Samples	Crystallinity (%)
Raw sugarcane bagasse	35.6
Holocellulose (delignified cellulose)	48.0
Chemically purified cellulose	63.5
Methylcellulose	43.7

The diffractogram corresponding to methylcellulose as compared to chemically purified cellulose shows diffraction peaks at the following 2θ angles: 8.2° and 20.2° as shown in Fig. 4(B). The presence of the peak at 8° is an evidence of modification of cellulose. The position of this peak indicates an increase of inter-planar distance in relation to the original cellulose (Filho et al., 2007). This occurs due to generation of disorder when the cellulose is modified. The projection of the substituting groups along the axis (methyl groups) is associated with an increase in the interfibrillar distance. This shows 43.7% crystallinity which may be due to a heterogeneous structure with a blockwise distribution of substituents. The FTIR spectrum which shows an intermediate structure between cellulose and methylcellulose. The reduction in crystallinity is due to less intermolecular chain interactions. The crystallinity percentage at different stages is given in Table 3.

4.5. Topographical studies of pore distribution by image analysis

Electron microscopical investigations in details show the fine structures of the pores (sponge-, cell- or sphere-, channel-like). FE-SEM provides high resolution imaging at low accelerating voltages and images give a good three dimensional impression of the pore structure (as shown in Fig. 5(A)). Their contrast is widely dominated by local sample orientation and some kind of 'illumination' contrast (Ziel, Haus, & Tulke, 2008). Simple image analysis of the MC/PVA porous scaffold was measured by topographical microscopy using

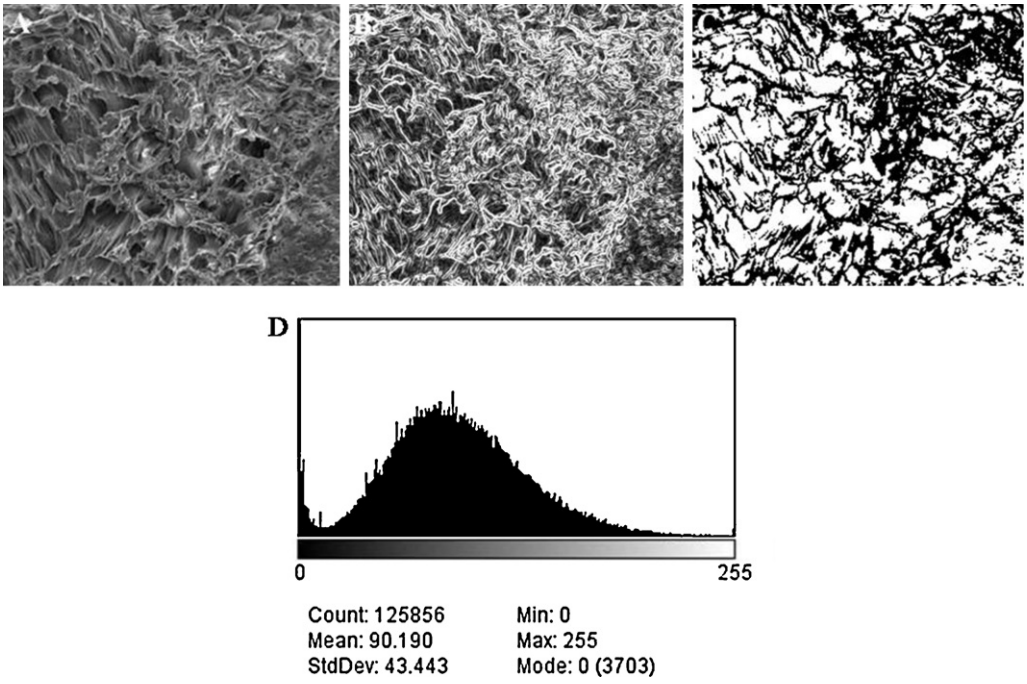

Fig. 5. Comparison of images obtained by (A) SEM, scale bar 500 μm, (B) sharp edge image, (C) binary application image analysis process in figure selective, and (D) topography pixel intensity histogram of methylcellulose/poly(vinyl alcohol) porous composite.

software ImageJ image processing (corresponding to a magnification of 100×).

Often pores are not in round shape. Because of this, pore size distribution cannot be measured manually. For this type of morphological structures, quantitative characterization should be in consideration. Pore distribution was detected by converting the more complex SEM image to a binary image showing only pores and the polymer matrix as shown in Fig. 5 (Mulinari et al., 2010; Ziel et al., 2008). Fig. 5(B) shows the sharp edges of the surface topography of the pore distribution and Fig. 5(C) shows the binary image showing the pores and the polymer matrix. The histogram of pore distribution was analyzed and shows the topography and rough surface of the porous composite (as shown in Fig. 5(D)). However, in order to investigate more quantitative data of surface and cross-section of porous composites, simple image analysis algorithms can be used to distinguish between pores and polymer.

5. Conclusions

Chemically purified α-cellulose was isolated from sugarcane bagasse and water soluble methylcellulose was prepared by methylation of α-cellulose using dimethyl sulfate (DMS) into acetone as solvent in a heterogeneous medium. A porous polymer composite was produced from a methylcellulose poly(vinyl alcohol) blend by freeze drying. FTIR data show the changes in structure due to the chemical treatments during synthesis and prove the modification of α-cellulose to methylcellulose. ^{1}H NMR confirmed the structure of the synthesized methylcellulose. X-ray diffraction (XRD) studies show structural support for the structure of methylcellulose with FTIR and ^{1}H NMR data and the changes in crystallinity during chemical treatments from raw sugarcane bagasse to chemically purified cellulose, and to synthesized methylcellulose were 35.6%, 63.5%, and 43.7%, respectively. The degree of substitution was calculated as 1.44. Scanning electron microscopy (SEM) images showed surface morphology of the samples. The porosity of porous composite was calculated as 86%. Image analysis of the porous composite investigated the topographical structure of the pores distribution having bizarre shapes and enhances its applicability for quantitative analysis of pore size distribution of the porous structures. 3D porous composite thus obtained may be applied in the biomedical area.

Acknowledgment

One of the authors, Mr. Anuj Kumar is highly thankful to the Ministry of Human Resource Development (MHRD), New Delhi for financial support during his PhD program.

References

Abe, K., Iwamoto, S., & Yano, H. (2007). Obtaining cellulose nanofibres with a uniform width of 15 nm from wood. *Biomacromolecules*, *8*, 3276–3278.

Abe, K., & Yano, H. (2009). Comparison of the characteristics of cellulose microfibril aggregates of wood, rice straw, and potato tuber. *Cellulose*, *16*, 1017–1023.

Bhatt, N., Gupta, P. K., & Naithani, S. (2011). Hydroxypropyl cellulose from a-cellulose isolated from *Lantana camara* with respect to DS and rheological behavior. *Carbohydrate Polymers*, *86*, 1519–1524.

Burczak, K. E., Gamian, E., & Kochman, A. (1996). Long-term in vivo performance and biocompatibility of poly (vinyl alcohol) hydrogel macrocapsules for hybrid type artificial pancreas. *Biomaterials*, *17*, 2351–2356.

Chakraborty, S., Chowdhury, S., & Saha, P. D. (2011). Adsorption of Crystal Violet from aqueous solution onto NaOH-modified rice husk. *Carbohydrate Polymers*, *86*, 1533–1541.

Chen, W. S., Yu, H. P., Liu, Y. X., Chen, P., Zhang, M. X., & Hai, Y. F. (2011). Individualization of cellulose nanofibres from wood using high-intensity ultrasonication combined with chemical pretreatments. *Carbohydrate Polymers*, *83*, 1804–1811.

Chhatri, A., Bajpai, A. K., Sandhu, S. S., Jain, N., & Biswas, J. (2011). Cryogenic fabrication of savlon loaded macroporous blends of alginate and polyvinyl alcohol (PVA), swelling, deswelling and antibacterial behaviors. *Carbohydrate Polymers*, *83*, 876–882.

Colom, X., Carrillo, F., Nogues, F., & Garriga, P. (2003). Structural analysis of photodegraded wood by means of FTIR spectroscopy. *Polymer Degradation and Stability*, *80*, 543–549.

Donges, R. (1990). Non-ionic cellulose ethers. *British Polymer Journal*, *23*, 315–326.

Filho, G. R., de Assuncao, R. M. N., Vieira, J. G., Meireles, C. S., Cerqueira, D. A., Barud, H. S., et al. (2007). Characterization of methylcellulose produced from sugarcane bagasse cellulose: Crystallinity and thermal properties. *Polymer Degradation and Stability*, *92*, 205–210.

Finch, C. A. (1973). *Polyvinyl alcohol: Properties and applications*. New York: Wiley Interscience.

Fu, X., & Chung, D. D. L. (1996). Effect of methylcellulose admixture on the mechanical properties of cement. *Cement and Concrete Research*, *26*, 535–538.

Giusti, P., Lazzeri, L., & Barbani, N. J. (1993). Hydrogels of poly (vinyl alcohol) and collagen as new bioartificial materials. *Journal of Materials Science: Materials in Medicine*, *4*, 538–542.

Habibi, Y., Lucia, L. A., & Rojas, O. J. (2010). Cellulose nanocrystals: Chemistry, self-assembly, and applications. *Chemical Reviews*, *110*, 3479–3500.

Hassan, C. M., & Peppas, N. A. (2000a). Structure and applications of poly (vinyl alcohol) hydrogels produced by conventional crosslinking or by freezing/thawing methods. *Advances in Polymer Science*, *153*, 37–65.

Hassan, C. M., & Peppas, N. A. (2000b). Cellular PVA hydrogels produced by freeze/thawing. *Journal of Applied Polymer Science*, *76*, 2075–2079.

Hoffman, A. S. (2002). Hydrogels for biomedical applications. *Advanced Drug Delivery Reviews*, *43*, 3–12.

Inoue, K., Fujisato, T., Gu, Y. J., Burezak, K., Sumi, S., Kogire, M., et al. (1992). Experimental hybrid islet transplantation: Application of poly (vinyl alcohol) membrane for entrapment of islets. *Pancreas*, *7*, 562–568.

Just, E. K., & Majewicz, T. G. (1985). Cellulose ethers. *Encyclopedia of Polymer Science and Engineering*, *3*.

Lee, K. Y., & Mooney, D. J. (2001). Hydrogels for tissue engineering. *Chemical Reviews*, *101*, 1869–1880.

Mansour, O. Y., Nagaty, A., & El-Zawawy, W. K. (1994). Variables affecting the methylation reactions of cellulose. *Journal of Applied Polymer Science*, *54*, 519–524.

Mansur, H. S., Sadahira, C. M., Souza, A. N., & Mansur, A. A. P. (2008). FTIR spectroscopy characterization of poly (vinyl alcohol) hydrogel with different hydrolysis degree and chemically crosslinked with glutaraldehyde. *Materials Science and Engineering C*, *28*, 539–548.

Mitchel, K., Ford, J. L., Armstrong, D. J., Elliot, P. N. C., Hogan, J. E., & Rostron, C. (1993). The influence of substitution type on the performance of methylcellulose and hydroxypropylmethylcellulose in gels and matrices. *International Journal of Pharmaceutics*, *100*, 143–154.

Morais, L. S., & Campana Filho, S. P. (1999). Carboximetilacao de polpas de Bagaco de cana d acucar e caracterizacao dos materiais absoventes obtidos. *Polimeros: Ciencia e Tecnologia*, *99*, 46–51.

Mulinari, D. R., Cruz, T. G., Cioffi, M. O. H., Voorwald, H. J. C., Da Silva, M. L. C. P., & Rocha, G. J. M. (2010). Image analysis of modified cellulose fibres from sugarcane bagasse by zirconium oxychloride. *Carbohydrate Research*, *345*, 1865–1871.

Nikitin, N. I. (1962). Cellulose ethers. In *The chemistry of cellulose and wood* (pp. 307–358).

Nishiyama, Y., Langan, P., & Chanzy, H. (2002). Crystal structure and hydrogen-bonding system in cellulose Iβ from synchrotron X-ray and neutron fibre diffraction. *Journal of American Chemical Society*, *124*, 9074–9082.

Nishiyama, Y., Sugiyama, J., Chanzy, H., & Langan, P. (2003). Crystal structure and hydrogen-bonding system in cellulose Iα from synchrotron X-ray and neutron fibre diffraction. *Journal of American Chemical Society*, *125*, 14300–14306.

Park, S., Baker, J. O., Himmel, M. E., Parilla, P. A., & Johnson, D. K. (2010). Cellulose crystallinity index: Measurement techniques and their impact on interpreting cellulase performance. *Biotechnology for Biofuels*, *3*, 1–10.

Pereira, P. H. F., Voorwald, H. C. J., Cioffi, M. O. H., Mulinari, D. R., Luz, S. M. D., & Da Silva, M. L. C. P. (2011). Sugarcane bagasse pulping and bleaching: Thermal and chemical characterization. *BioResources*, *6*, 2471–2482.

Peresin, M. S., Habibi, Y., Zoppe, J. O., Pawlak, J. J., & Rojas, O. J. (2010). Nanofibre composites of polyvinyl alcohol and cellulose nanocrystals: Manufacture and characterization. *Biomacromolecules*, *11*, 674–681.

Razzak, M. T., Zainuddin, E., Dewi, S., Lely, H., & Taty, S. (1999). The characterization of dressing component materials and radiation formation of PVA-PVP hydrogel. *Radian Physics and Chemistry*, *55*, 153–165.

Reibert, K. C., & Conklin, J. R. (1999). USPTO – US Patent 6,235,893.

Ripoli, C. C., Molina, W. F., Jr., & Ripoli, M. L. C. (2000). Energy potential of sugarcane biomass in Brazil. *Scientia Agricola*, *57*, 677–681.

Rodrigues Filho, G., Cruz, S. F., Pasquini, D., Cerqueira, D. A., Prado, V. S., & de Assuncao, R. M. N. (2000). Water flux through cellulose triacetate films produced from heterogeneous acetylation of sugarcane bagasse. *Journal of Membrane Science*, *177*, 225–231.

Sekiguchi, Y., Sawatari, C., & Kondo, T. (2002). A facile method of detection for distribution of the substituent in *O*-methylcelluloses using ^{1}H-NMR spectroscopy. *Polymer Bulletin*, *47*, 547–554.

Sekiguchi, Y., Sawatari, C., & Kondo, T. (2003). A gelation mechanism depending on hydrogen bond formation in regioselectively substituted O-methylcelluloses. *Carbohydrate Polymers*, *53*, 145–153.

Sun, X. F., Sun, R. C., & Sun, J. X. (2004). Acetylation of sugarcane bagasse using NBS as a catalyst under mild reaction conditions for the production of oil sorption-active materials. *Bioresource Technology*, *95*, 343–350.

Tita, S. P. S., de Paiva, J. M. F., & Frollini, E. (2002). Resistencia ao Impacto e Outras Propriedades de Compositos Lignocelulosicos: Matrizes Termofixas Fenolicas Reforcadas com Fibras de Bagaco de Cana-de-acucar. *Polimeros: Ciencia e Tecnologia*, *12*, 228–233.

Viera, R. G. P., Filho, G. R., de Assuncao, R. M. N., Meireles, C. S., Vieira, J. G., & de Oliveira, G. S. (2007). Synthesis and characterization of methylcellulose from sugarcane bagasse cellulose. *Carbohydrate Polymers*, *67*, 182–189.

Viera, R. G. P., Meireles, C. S., de Assuncao, R. M. N., & Rodrigues Filho, G. (2004). Production and characterization of methylcellulose from sugarcane bagasse. In *Proceedings of 5th international symposium on natural polymers and composites, 8th Brazilian symposium on the chemistry of lignins and the other wood components* Sao Pedro – SP, Brazil, (pp. 1–3).

Wan, W. K., Campell, G., Zhang, Z. F., Hui, A. J., & Boughner, D. R. (2002). Optimizing the tensile properties of poly (vinyl alcohol) hydrogel for the construction of a bioprosthetic heart valve stent. *Journal of Biology Matters Research*, *63*, 854–861.

Young, T. H., Chuang, W. Y., Yao, N. K., & Chen, L. W. (1998). Use of diffusion model for assessing the performance of poly (vinyl alcohol) bioartificial pancreases. *Journal of Biomedical Materials Research*, *40*, 385–391.

Zhbankov, R. G. (1966). *Infrared spectra of cellulose and its derivatives*. New York: Plenum Publishing Corporation.

Ziel, R., Haus, A., & Tulke, A. (2008). Quantification of the pore size distribution (porosity profiles) in microfiltration membranes by SEM, TEM, and computer image analysis. *Journal of Membrane Science*, *323*, 241–246.

Zohuriaan, M. J, & Shokrolahi, F. (2004). Thermal studies on natural and modified gums. *Polymer Testing*, *23*, 575–579.